



ELSEVIER

Contents lists available at SciVerse ScienceDirect

## Journal of Fluids and Structures

journal homepage: [www.elsevier.com/locate/jfs](http://www.elsevier.com/locate/jfs)

# Panel flutter at low supersonic speeds

Vasily V. Vedeneev\*

Lomonosov Moscow State University, 1, Leninskie Gory, Moscow, Russia

## ARTICLE INFO

### Article history:

Received 30 December 2010

Accepted 28 December 2011

Available online 31 January 2012

### Keywords:

Panel flutter

Plate flutter

Single mode flutter

Single degree of freedom flutter

## ABSTRACT

Flutter of panels can be of two possible types: single mode or coupled mode flutter. Coupled mode flutter has been thoroughly studied using piston theory, which represents air pressure acting on the plate at high Mach numbers. Single mode flutter cannot be studied using piston theory and requires potential flow theory or more complex aerodynamic theories. This type of flutter occurs at low supersonic Mach numbers and is studied insufficiently. In this paper a comprehensive numerical investigation of single mode flutter is conducted to perform study of flutter boundaries and their transformations due to changes within the problem parameters.

© 2012 Elsevier Ltd. All rights reserved.

## 1. Introduction

Panel flutter is a phenomenon of self-exciting vibrations of skin panels of flight vehicle at high flight speeds. Such vibrations typically have high amplitude and cause fatigue damage of skin panels. This flutter phenomenon was first observed during World War II; however, formal studies did not appear until the 1950s. From a mathematical point of view, the problem of panel flutter can be studied through spectral problem for equation of plate motion in a gas flow:

$$\mathcal{D} \frac{\partial^4 w}{\partial x^4} - \sigma h \frac{\partial^2 w}{\partial x^2} + \rho_m h \frac{\partial^2 w}{\partial t^2} + p(x, t) = 0, \quad (1)$$

supplemented by appropriate boundary conditions at  $x=0, \mathcal{L}$ . Here  $\mathcal{D}$ ,  $\mathcal{L}$  and  $h$  are plate stiffness, length and thickness, respectively,  $\rho_m$  is plate material density,  $p$  is unsteady gas pressure caused by plate deflection  $w$ . We assume that the plate is stretched with in-plane tension stress  $\sigma > 0$ . The pressure obtained from potential gas flow theory is a complicated integro-differential expression in terms of  $w$  (see formula (6) below); however, in 1956 a simple approximation of the pressure as  $M \rightarrow \infty$ , called “piston theory”, was derived

$$p(x, t) = \frac{\rho u}{\sqrt{M^2 - 1}} \left( \frac{\partial w}{\partial t} + u \frac{\partial w}{\partial x} \right), \quad (2)$$

where  $\rho$ ,  $u$  and  $M$  are the flow density, speed and Mach number. The partial-differential equation resulting from the problem (1), (2) has been studied in detail analytically (Movchan, 1956, 1957) and numerically (Bolotin, 1963; Dugundji, 1966; Hedgepeth, 1957). Many studies conducted since piston theory was derived, deal with different complications from the elastic portion of the problem: nonlinear plate models (Bolotin, 1960, 1963; Dowell, 1966, 1974; Mei et al., 1999), plates made of composite materials and shape memory alloys (Abdel-Motagaly et al., 1999; Bohon, 1963; Duan et al., 2003; Zhou et al., 1995), chaotic vibrations of buckled and pre-stressed plates (Bolotin et al., 1998; Dowell, 1982).

\*Tel.: +7 916 338 23 82.

E-mail address: [vasily@vedeneev.ru](mailto:vasily@vedeneev.ru)

URL: <http://www.vedeneev.ru>

## Nomenclature

$a$	speed of sound of the gas flow
$E$	Young's modulus of plate material
$\mathcal{D}$	$Eh^3/(12(1-\nu^2)) =$ plate bending stiffness
$D$	$\mathcal{D}/(a^2 \rho_m h^3) = E/(12(1-\nu^2)a^2 \rho_m) =$ dimensionless plate stiffness
$h$	plate thickness
$\mathcal{L}$	plate length
$L$	$\mathcal{L}/h =$ dimensionless plate length
$M$	$u/a =$ Mach number
$M_w$	$\sqrt{\sigma/\rho_m}/a =$ dimensionless propagation speed of long plate waves, this parameter is a characteristic of the plate tension
$u$	gas flow speed
$w$	dimensionless (except Introduction) vertical plate deflection, nondimensionalized by $h$
$\mu$	$\rho/\rho_m =$ dimensionless gas density
$\nu$	Poisson's ratio of plate material
$\rho$	gas density
$\rho_m$	plate material density
$\sigma$	in-plane tension stress of the plate
$\omega$	dimensionless frequency, nondimensionalized by $a/h$

However, the studies to date have typically not changed aerodynamic portion of the problem, piston theory (2), due to high complexity of the exact potential flow theory.

Piston theory initially was obtained as an asymptotic expansion of the exact expression as  $M \rightarrow \infty$ . In later studies it was shown that piston theory is valid starting from  $M \approx 1.7$  (Bolotin, 1963). Thus, it does not cover the range of low supersonic Mach number,  $1 < M < 1.7$ . Few papers among large amount of publications were devoted to study of panel flutter problem using potential flow theory or more complex theories: Nelson and Cunningham (1956), Dun Min-de (1958), Dowell and Voss (1965), Dowell (1967, 1971, 1974), Yang (1975), Dong Ming-de (1984), Bendiksen and Davis (1995), Selvam et al. (1998), Gordnier and Visbal (2001), and Hashimoto et al. (2009). In those studies occurrence of single mode flutter (also known as single degree of freedom flutter) at low supersonic speeds was noticed, in contrast to coupled mode flutter (also referred as coalescence flutter), which arises at higher  $M$ . Coupled mode flutter has been thoroughly studied through piston theory; it occurs due to interaction of two plate eigenmodes. Single mode flutter is often considered as a consequence of negative aerodynamic damping. Indeed, expansion of pressure derived from potential flow theory at low frequencies yields

$$p(x,t) = \frac{\rho u}{\sqrt{M^2-1}} \left( \frac{M^2-2}{M^2-1} \frac{\partial w}{\partial t} + u \frac{\partial w}{\partial x} \right). \quad (3)$$

Coefficient of  $\partial w/\partial t$ , which represents aerodynamic damping, is negative if  $M < \sqrt{2}$ , and in this case (3) always predicts single mode instability. However, using this simplistic approach to investigate single mode flutter results in contradictory conclusions, such as flutter response is predicted in all plate eigenmodes with any in-plane plate loading and for any plate lengths (even very short plates). Also for nonlinear plate models, expression (3) is inadequate for analysis of limit cycle oscillations because amplitude growth becomes unlimited. Detailed study of single mode flutter through potential flow theory or more complex theories has never been conducted, due to great complexity of the mathematical problem. Also, there has been some bias in conviction, within the research being performed to date, to gloss over this type of flutter as not able to occur in physical reality and on actual structures.

Over the last years Vedenev (2005, 2006) studied single mode flutter of long plates using asymptotic theory of global instability (Kulikovskii, 1966, 2006), never previously used in aeroelasticity. Note that Kulikovskii's theory of global instability has been successfully used in related fields (Doaré and de Langre, 2006; Peake, 2004). The asymptotic flutter criterion has been obtained as the plate length  $\mathcal{L} \rightarrow \infty$ . The energy transfer mechanism between the plate and the flow has been studied in detail. Theoretical study of limit cycle amplitude of single mode flutter (Vedenev, 2007) has shown that increase of amplitude while entering flutter region in the parameter space is much more rapid than for coupled mode flutter. Recent experimental study (Vedenev et al., 2010) has confirmed by demonstration that single mode flutter can occur in real structures.

In this paper we conduct comprehensive numerical investigation of two-dimensional panel flutter problem using potential gas flow theory. From mathematical point of view, this problem is equivalent to those considered in Nelson and Cunningham (1956) and Yang (1975). However, several important characteristic features of single mode flutter were unnoticed by previous studies but have been uncovered by Vedenev (2005), including such items as: flutter boundaries are not influenced by gas density (this result is in contrast to coupled mode flutter, which is highly dependent on gas density), instability can occur in several eigenmodes simultaneously, existence of asymptotic flutter boundaries for long plates, and effectiveness of plate tension to provide action on flutter boundaries. In order to conduct detailed investigation

of such features, we will consider larger number of eigenmodes with wider variation of the parameters, than in earlier studies.

Note that, as the problem is two-dimensional, the panel is considered to have an infinite aspect ratio. For rectangular panels of medium and small aspect ratios single mode flutter region is generally smaller or may even disappear (Dowell, 1974). Thus, results of this paper are applicable to panels of high aspect ratios, whereas case of low aspect ratios is a topic for future studies.

## 2. Formulation of the problem

We consider linear stability of elastic plate in a uniform gas flow. Elastic properties of the plate are defined by the parameters  $\mathcal{D}$ ,  $\mathcal{L}$ ,  $h$ , and  $\rho_m$ ; flow parameters are the flow speed  $u$ , speed of sound  $a$ , and the flow density  $\rho$ . For nondimensionalization we choose dimensionally independent parameters  $a$ ,  $\rho$  and  $h$ , then dimensionless variables are

$$D = \frac{\mathcal{D}}{a^2 \rho_m h^3}, \quad M_w = \frac{\sqrt{\sigma/\rho_m}}{a}, \quad L = \frac{\mathcal{L}}{h}, \quad M = \frac{u}{a}, \quad \mu = \frac{\rho}{\rho_m}.$$

This choice of dimensionless parameters is not typical in aeroelasticity, nevertheless, it is very efficient in study of single mode flutter. First, the plate length  $\mathcal{L}$  and thickness  $h$  are not included into any parameter except  $L$  (indeed,  $\mathcal{D} = Eh^3/(12(1-\nu^2))$ , therefore  $D$  can be cancelled by  $h^3$ ), which makes possible asymptotic study as  $L \rightarrow \infty$ . Second, gas density  $\rho$  is not included into any parameter except  $\mu$ , which is typically very small. This allows to use  $\mu$  as a small parameter in asymptotic analysis (Vedenev, 2005, 2006), which yields the following result: single mode flutter boundaries do not depend on  $\mu$ . It can be difficult to prove this results if other dimensionless parameters are chosen. Below we will confirm the independence from gas density as a contributing factor for the single mode flutter problem for arbitrary plate length.

The plate is mounted into an infinite absolutely rigid plane. Gas flow occupies the upper half-plane, while in the lower half-plane constant pressure equal to undisturbed flow pressure is set (Fig. 1). Using the dimensionless variables, rewrite (1)

$$D \frac{\partial^4 w}{\partial x^4} - M_w^2 \frac{\partial^2 w}{\partial x^2} + \frac{\partial^2 w}{\partial t^2} + p(x,t) = 0,$$

where plate deflection  $w$  is nondimensionalized by  $h$ .

Consider harmonic motion of the plate,  $w(x,t) = W(x)e^{-i\omega t}$ , then substitution in the equation yields

$$D \frac{d^4 W}{dx^4} - M_w^2 \frac{d^2 W}{dx^2} - \omega^2 W + p\{W, \omega\} = 0. \tag{4}$$

Unsteady gas pressure obtained from potential flow theory (Bolotin, 1963; Garric and Rubinow, 1946; Miles, 1959; Nelson and Cunningham, 1956) has the form

$$p\{W, \omega\} = \frac{\mu}{\sqrt{M^2 - 1}} \left( -i\omega + M \frac{d}{dx} \right) \int_0^x \left( -i\omega W(\xi) + M \frac{dW(\xi)}{d\xi} \right) \exp\left( \frac{iM\omega(x-\xi)}{M^2 - 1} \right) J_0\left( \frac{-\omega(x-\xi)}{M^2 - 1} \right) d\xi, \tag{5}$$

which transforms to

$$p\{W, \omega\} = \frac{\mu M}{\sqrt{M^2 - 1}} \left( -i\omega W(x) + M \frac{dW(x)}{dx} \right) + \frac{\mu \omega}{(M^2 - 1)^{3/2}} \int_0^x \left( -i\omega W(\xi) + M \frac{dW(\xi)}{d\xi} \right) \times \exp\left( \frac{iM\omega(x-\xi)}{M^2 - 1} \right) \left( iJ_0\left( \frac{-\omega(x-\xi)}{M^2 - 1} \right) + MJ_1\left( \frac{-\omega(x-\xi)}{M^2 - 1} \right) \right) d\xi. \tag{6}$$

We will consider plates simply supported at both edges, therefore

$$W = \frac{d^2 W}{dx^2} = 0, \quad x = 0, \quad x = L. \tag{7}$$

The problem (4), (6), (7) is eigenvalue problem for the plate in the gas flow. If at least one eigenfrequency  $\omega_n$  has positive imaginary part, then the plate flutters; otherwise the plate is stable.

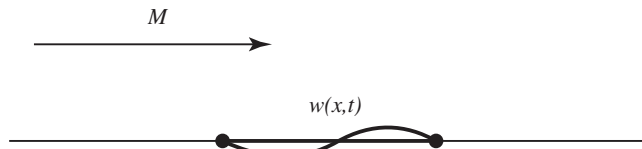


Fig. 1. Plate in supersonic gas flow.

Piston theory (2) can be obtained by omitting integral term in (6):

$$p\{W, \omega\} = \frac{\mu M}{\sqrt{M^2 - 1}} \left( -i\omega W(x) + M \frac{dW(x)}{dx} \right). \quad (8)$$

We will use piston theory (8) for comparison with results obtained through potential flow theory (6).

Note that similar problem was recently studied by Banichuk et al. (2011). However, they considered moving plate in incompressible fluid, so that plate equation was slightly changed compared to (4), also kernel function of unsteady pressure (5) was different and did not depend on  $\omega$ .

### 3. Numerical method

#### 3.1. Formulation of the numerical procedure

We will use Galerkin method for analysis of the problem. Basic functions are normal mode shapes of the plate in vacuum:

$$W(x) = \sum_{n=1}^N C_n W_n(x), \quad W_n(x) = \sin\left(\frac{n\pi x}{L}\right),$$

where  $C_n$  are unknown constants. By substituting this expression into (4), multiplying by  $W_m(x)$ ,  $m = 1, \dots, N$ , and integrating from 0 to  $L$ , we obtain a homogeneous system of algebraic equations with unknowns  $C_n$ . Matrix of this system is

$$\mathbf{A}(\omega) = \mathbf{K} + \mathbf{P}(\omega) - \frac{L\omega^2}{2} \mathbf{I},$$

where  $\mathbf{K}$  is the diagonal stiffness matrix with coefficients

$$k_{jj} = \left( D \left( \frac{j\pi}{L} \right)^4 + M_w^2 \left( \frac{j\pi}{L} \right)^2 \right) \frac{L}{2}, \quad k_{jn} = 0, \quad j \neq n;$$

$\mathbf{P}$  is the aerodynamic force matrix with coefficients

$$p_{jn}(\omega) = \int_0^L P\{W_n, \omega\} \cdot W_j \, dx, \quad (9)$$

$\mathbf{I}$  is the unit matrix. Frequency equation, therefore, takes the form

$$\det \mathbf{A}(\omega) = \det \left( \mathbf{K} + \mathbf{P}(\omega) - \frac{L\omega^2}{2} \mathbf{I} \right) = 0. \quad (10)$$

Matrix  $\mathbf{P}(\omega)$  is complex and non-symmetric, with all coefficients non-zero. Therefore, the problem is not self-adjointed, and solutions of (10) are complex.

Iterative method is used for solving (10). Assume that we calculate  $n$ -th eigenfrequency  $\omega_n$ . As initial condition, we use natural frequency of the plate in vacuum:  $\omega_n^0 = \sqrt{D(n\pi/L)^4 + M_w^2(n\pi/L)^2}$ . Next, let us have  $p$ -th approximation  $\omega_n^p$ . Define matrix  $\mathbf{A}_{p+1}(\omega_n^p, \omega_n^{p+1})$  as follows, where  $\omega_n^{p+1}$  is an auxiliary value used to calculate  $\omega_n^{p+1}$ . All coefficients  $a_{jk}$ , except  $a_{nn}$ , are the same as of matrix  $\mathbf{A}(\omega_n^p)$ , while for  $a_{nn}$  we use the following expression:

$$a_{nn} = k_{nn} + p_{nn}(\omega_n^p) - \frac{L(\omega_n^{p+1})^2}{2}, \quad (11)$$

where  $k_{nn}$  and  $p_{nn}$  are the appropriate coefficients of matrixes  $\mathbf{K}$  and  $\mathbf{P}$ .

The equation for  $\omega_n^{p+1}$  is

$$\det \mathbf{A}_{p+1}(\omega_n^p, \omega_n^{p+1}) = 0;$$

it is linear with respect to  $(\omega_n^{p+1})^2$ . Among two values of  $\omega_n^{p+1}$  we choose the one with positive real part:  $\text{Re } \omega_n^{p+1} > 0$ .

Finally, we calculate  $p+1$ -th approximation of  $\omega_n$  as follows:

$$\omega_n^{p+1} = (1-\alpha)\omega_n^{p+1} + \alpha\omega_n^p,$$

where  $\alpha$  is the relaxation coefficient,  $0 \leq \alpha < 1$ .

Iterative procedure described typically converges (see Section 3.2 below for details). However, at high  $M$  and  $L$ , when coupled mode flutter is the primary type of instability, such a procedure could diverge. This usually happens when the first and the second eigenfrequencies are close to each other and almost coalesce, such that the numerical solution at each iteration may “jump” from one value to another. In this case expression (11) was used for both  $a_{11}$  and  $a_{22}$ . Hence, equation for  $\omega_n^{p+1}$ ,  $n=1, 2$  is quadratic with respect to  $(\omega_n^{p+1})^2$  and gives both first and second eigenvalues, which allows to easily distinguish them and follow the same eigenvalue at each iteration.

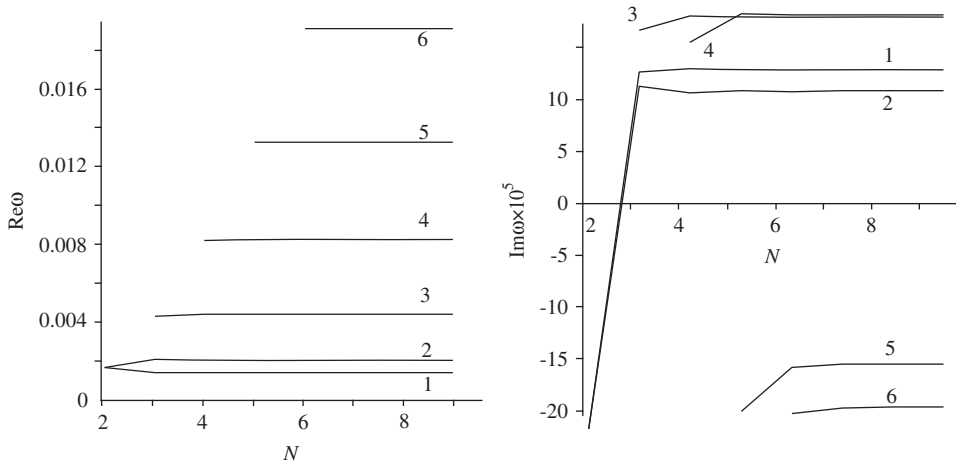


**Fig. 2.** Convergence of  $\omega_n$  iterations ( $n = 1, \dots, 6$ ) with increase of number of basic modes  $N$  for parameters (12),  $M=1.2$ ,  $L=300$ .

Iterations for  $\omega_n$  continue until the following convergence criterion is satisfied:

$$\frac{\omega_n^p - \omega_n^{p-1}}{\omega_n^p} < \varepsilon_1.$$

After the convergence criterion has been achieved, the condition  $\det \mathbf{A}(\omega_n^p) < \varepsilon_2$  is checked.

Inside of each iteration only matrix  $\mathbf{P}(\omega_n^p)$  is calculated numerically. Each coefficient  $p_{jk}(\omega_n^p)$  requires calculation of two integrals: inner one (6) and outer one (9). The inner integral is calculated using Simpson’s rule, the outer one is calculated using trapezoidal rule.

### 3.2. Convergence of the numerical procedure

Now we will study convergence and robustness of the numerical method described. First, let us consider number of basic functions,  $N$ , necessary to obtain accurate solution. Shown in Fig. 2 are real and imaginary parts of the first six eigenfrequencies for parameters

$$D = 23.9, \quad M_w = 0, \quad \mu = 12 \times 10^{-5}, \tag{12}$$

$M=1.2$ ,  $L=300$  (these parameters correspond to a steel plate in air flow at 3000 m above sea level). Maximum residual  $\varepsilon_1 = 10^{-5}$  and relaxation coefficient  $\kappa = 0.5$  are used. It is seen that  $N = n + 1$  modes is enough to calculate  $\omega_n$  with high accuracy, such that relative error of both  $\text{Re } \omega_n$  and  $\text{Im } \omega_n$  is less than 1%. In this paper we will study the first six modes; therefore,  $N=7$  is enough to get appropriate accuracy. This stays true for any medium-size plates,  $L < 600$ . For higher  $L$  more modes are necessary. For the first six modes,  $N=9$  gives better solution for  $L \approx 600$ ,  $N=11$  for  $L \approx 700$ , and  $N=13$  for  $L \approx 800$ .

Next, in Fig. 3 calculated  $\omega_n$  versus maximum residual  $\varepsilon_1 = 10^{-1}, \dots, 10^{-9}$  are shown, relaxation coefficient  $\kappa = 0.5$  is used. It is seen that  $\varepsilon_1 = 10^{-5}$  is typically enough to get relative error less than 1% for  $n = 1, \dots, 6$ . We will use this value in all further calculations.

Finally, in Fig. 4 influence of relaxation coefficient  $\kappa$  is shown. For  $\kappa = 0$  at low  $M > 1$  the iterative process for the first two eigenfrequencies converges very slowly. Use of  $\kappa = 0.25$  and  $0.5$  forces convergence, however higher  $\kappa$  reduces convergence rate at higher  $M$  (it is obvious that convergence is very slow, as  $\kappa \rightarrow 1$ , due to small change of  $\omega_n^p$  at each iteration). For  $n > 2$  convergence of  $\omega_n$  is much faster for any  $\kappa$  (that is why higher modes are not shown in Fig. 4); thus  $n = 1, 2$  are the critical modes. For higher plate lengths ( $L > 400$ ) distances between eigenfrequencies in the complex plane become smaller, and the iterative procedure may converge slower or even diverge, “jumping” from one eigenfrequency to another. In this case  $\kappa = 0.7$  gives more robust and faster convergence. Further for all calculations we will use  $\kappa = 0.0, \dots, 0.7$ , depending on the plate size and the current convergence rate.

## 4. Closed-form asymptotic solution for long plates

Before proceeding to results of calculations, let us consider flutter properties discovered in asymptotic study (Vedenev, 2005). The problem has a large parameter  $L$  and a small parameters  $\mu$ . Using theory of global instability (Kulikovskii, 1966, 2006), flutter boundaries have been obtained as  $L \rightarrow \infty$  and  $\mu \rightarrow 0$ .

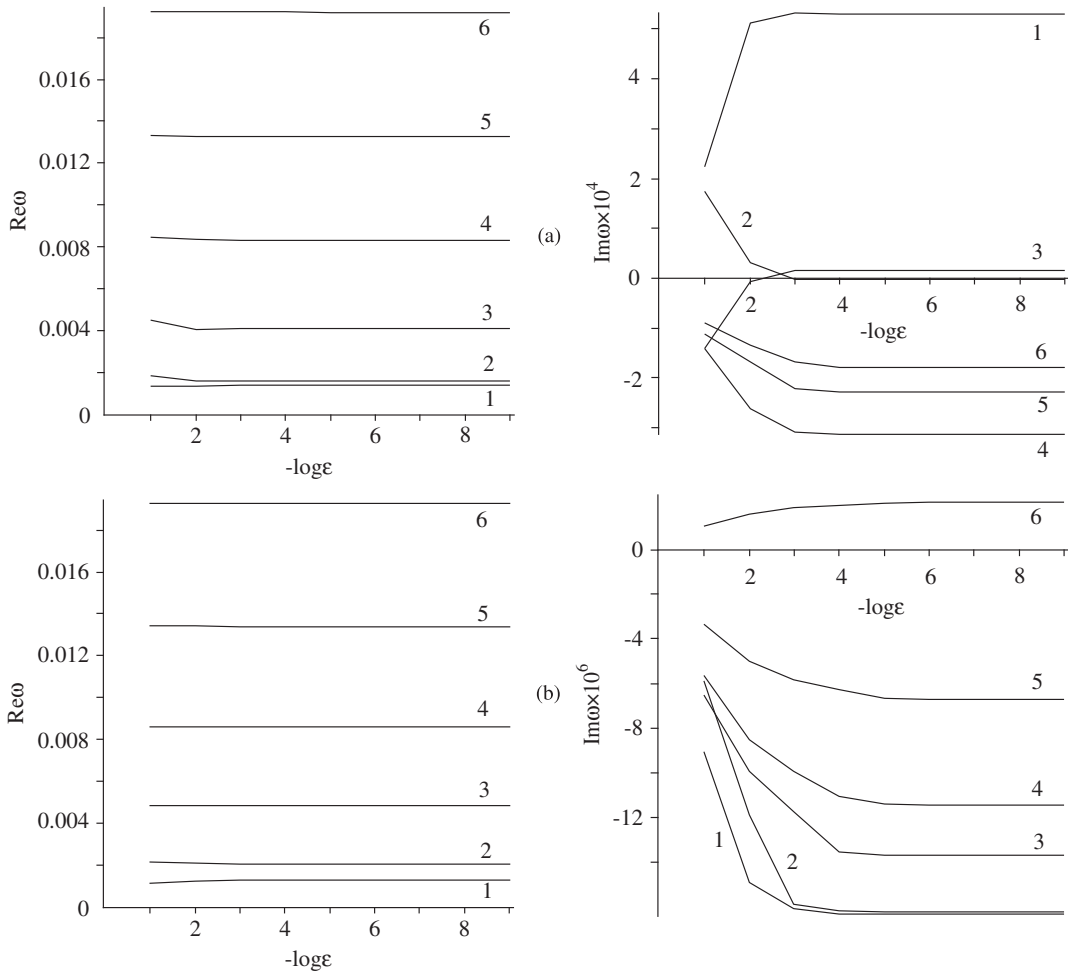


**Fig. 3.** Convergence of  $\omega_n$  iterations ( $n=1, \dots, 6$ ) with decrease of maximum residual  $\epsilon_1 = 10^{-1}, \dots, 10^{-9}$  for parameters (12),  $L=300$ . (a)  $M=1.1$ , (b)  $M=1.5$ .

The main idea of this theory is as follows. We are looking for solutions of the system in the form

$$W(x) = \sum_{j=1}^4 e^{ik_j x}. \tag{13}$$

Each term here represents a wave running along the plate, however superposition (13) can be either standing or running wave. Each wave number  $k_j = k_j(\omega)$  is one of the four solutions of dispersion equation for infinite plate-flow system

$$Dk^4 + M_w^2 k^2 - \omega^2 - \mu \frac{(\omega - Mk)^2}{\sqrt{k^2 - (\omega - Mk)^2}} = 0. \tag{14}$$

First three terms here represent elastic and mass properties of the plate, while the last term represents the gas flow. Investigation of branch points and cuts of  $k_j(\omega)$  shows that these four solutions are analytic continuations of branches that satisfy (14) at  $\text{Im } \omega \gg 1$  for  $\text{Re} \sqrt{k^2 - (\omega - Mk)^2} > 0$  (radiation condition). Numbering of  $k_j$  is such that  $\text{Im } k_1 > \text{Im } k_2 > \text{Im } k_3 > \text{Im } k_4$  for  $\text{Im } \omega \gg 1$ . For real  $\omega$ , two of these solutions tend to imaginary numbers as  $\mu \rightarrow 0$  and correspond to spatially damping waves as  $x \rightarrow +\infty$  or  $x \rightarrow -\infty$ . Two other solutions tend to real numbers as  $\mu \rightarrow 0$  and correspond to harmonic waves.

Substitution of (13) into the boundary conditions yields the frequency equation. Kulikovskii (1966) proved that as  $L \rightarrow \infty$  this equation has asymptotic form

$$\min_{j=1,2} \text{Im } k_j(\omega) = \max_{j=3,4} \text{Im } k_j(\omega). \tag{15}$$

This equation defines a curve  $\Omega$  in the complex  $\omega$ -plane, which does not depend neither on  $L$ , nor on boundary conditions assigned at the plate edges. Thus, this curve is attractor of discrete spectrum of eigenfrequencies for long plates

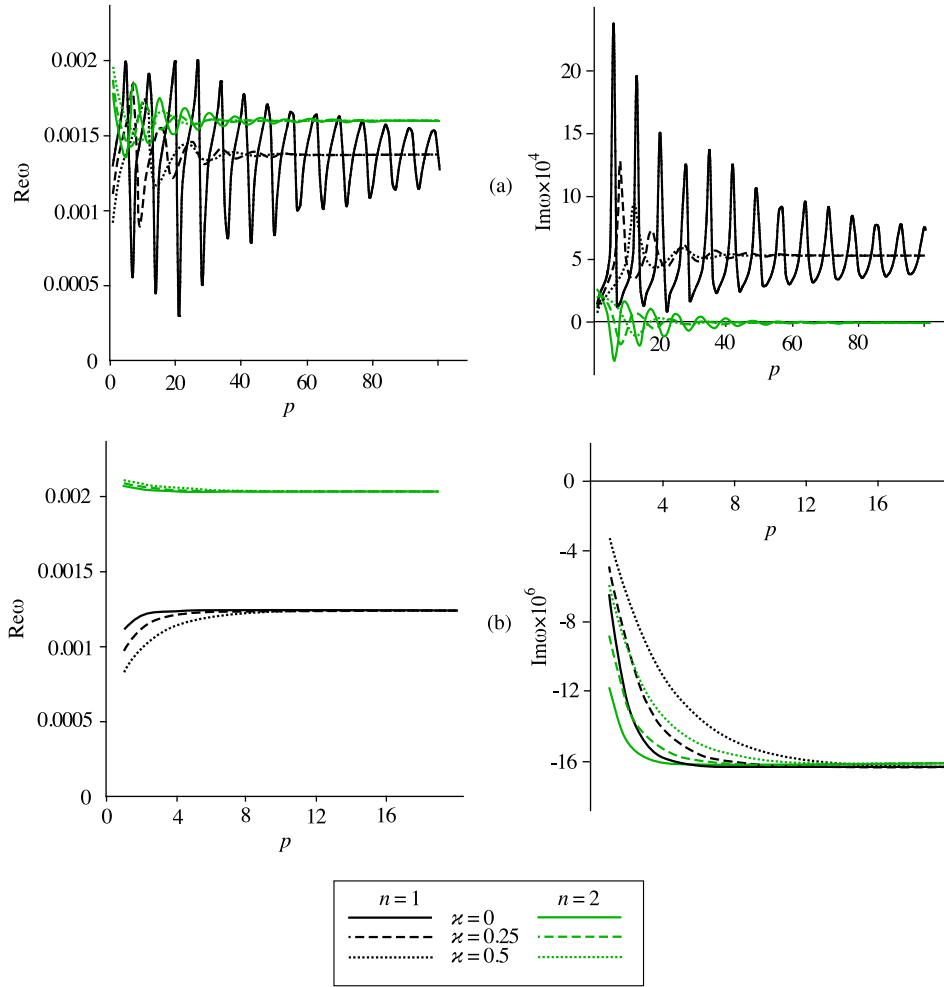


Fig. 4. Iterative process,  $\omega_n^p$ , for relaxation coefficients  $\zeta = 0, 0.25, 0.5$ , for parameters (12),  $L=300$ . (a)  $M=1.1$ , (b)  $M=1.5$ .

in a gas flow. With change of  $L$ , eigenfrequencies move along curve  $\Omega$ , staying in its neighbourhood. If some section of  $\Omega$  lies in region  $\text{Im } \omega > 0$ , then eigenfrequencies lying near this section have positive imaginary part, and the plate is unstable.

Vedenev (2005) showed that  $\Omega$  can have two distinct sections located in the upper half-plane, one section corresponds to single mode flutter, the other section corresponds to coupled mode flutter (Fig. 5). According to these two sections, there exist two regions of instability in parameter space of a plate in a gas flow. The first one is located in the lower  $M$  region, its asymptotic instability criterion is

$$M > M_w + 1.$$

Assuming that  $\text{Re } \omega_n$  in vacuum and in the gas flow are close (this is reasonable for single mode flutter, as  $\mu \ll 1$ ), detailed analysis yields instability criterion of each mode:  $n$ -th mode is unstable if

$$M_n^* < M < M_n^{**}, \tag{16}$$

where

$$M_n^* = 1 + \sqrt{\lambda_n}, \quad M_n^{**} = \sqrt{1 + \lambda_n + \sqrt{4\lambda_n + 1}}, \quad \lambda_n = \frac{\sqrt{4D\omega_{0n}^2 + M_w^4 + M_w^2}}{2}, \quad \omega_{0n} = \sqrt{D\left(\frac{\pi n}{L}\right)^4 + M_w^2\left(\frac{\pi n}{L}\right)^2}, \tag{17}$$

and  $\omega_{0n}$  is  $n$ -th natural frequency of the plate in vacuum. In the region (16) single-mode flutter occurs:  $n$ -th mode is unstable ( $\text{Im } \omega_n > 0$ ) independently on others, eigenfrequencies do not approach each other during transition to instability.

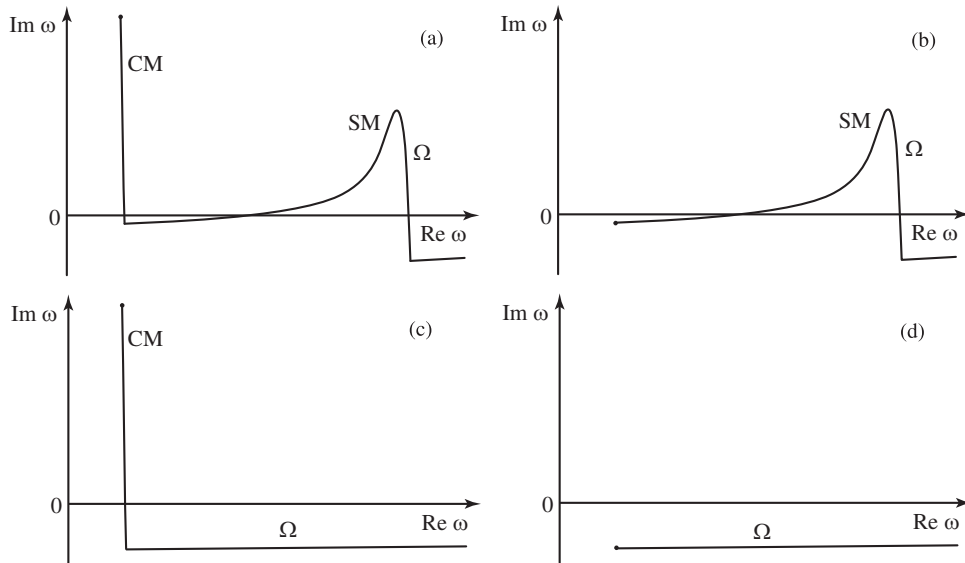


**Fig. 5.** Possible configurations of  $\Omega$ . (a) Single mode (SM) and coupled mode (CM) types of flutter, (b) only single mode type of flutter, (c) only coupled mode type of flutter, (d) stability.

At higher  $M$  there is a second region of instability, which has the following asymptotic form as  $L \rightarrow \infty$ :

$$M_w < \left(\frac{\sqrt{54}}{4}\right)^{1/3} \left(\mu \frac{M^2}{\sqrt{M^2-1}}\right)^{1/3} D^{1/6}. \quad (18)$$

This instability region corresponds to coupled mode flutter, where two or more eigenmodes interfere with each other during transition to flutter. Due to coalescence of eigenfrequencies, deriving asymptotic flutter boundaries of each mode is not possible without considering the full boundary value problem.

The most interesting feature of single mode flutter criterion (16) is that it does not contain dimensionless parameter  $\mu$ . This means that stability or instability itself does not depend on the flow density. However, if instability occurs in some eigenmode, its growth rate  $\text{Im } \omega_n$  is a function of  $\mu$ .

## 5. Results of calculations

Asymptotic results described in the previous section have two sources of inaccuracy. First, use of asymptotic frequency equation (15) instead of the full boundary value problem. Second, linear combination (13) satisfies all equations and boundary conditions, except the rigidity condition along the plane  $z=0$  before the plate:  $w(x,t)=0$ ,  $x < 0$ . Let us now consider results of numerical calculations of the full boundary value problem for arbitrary  $L$ .

### 5.1. Flutter boundaries and behaviour of eigenfrequencies

Analysis is conducted for a steel plate in air flow at 3000 m above sea level. The problem parameters are  $E = 2.11 \times 10^{11}$  Pa,  $\nu = 0.3$ ,  $\rho_m = 7500$  kg/m<sup>3</sup>,  $a = 328.6$  m/s,  $\rho = 0.91$  kg/m<sup>3</sup>. First, let us consider case of unstressed plate, corresponding dimensionless parameters are given by (12). Flutter boundaries obtained through exact potential flow theory are shown in Fig. 6 by dashed curves. Each eigenmode has its own flutter region in  $M-L$  plane. With increase of  $L$ , flutter critical Mach numbers  $M_n^*(L)$ ,  $M_n^{**}(L)$  decrease and tend to asymptotic values predicted by (17):  $M_n^* \rightarrow 1$ ,  $M_n^{**} \rightarrow \sqrt{2}$  as  $L \rightarrow \infty$ . At certain  $L$  (thick dashed curve in Fig. 6) coalescence of the first and second modes and following coupled mode flutter occur. This, however, does not affect third and higher modes, so that their single mode flutter boundaries extend to higher  $L$  region.

In order to understand nature of single mode and coupled mode instabilities, let us consider motion of eigenfrequencies in  $\omega$ -plane. For simplicity, we will watch only the first four eigenfrequencies, since the qualitative behaviour of the higher frequencies will be the same. For  $L=250$ ,  $M=1.6$  all the first six eigenfrequencies lie in the lower half-plane (Fig. 7), and the corresponding eigenmodes are damped. Keeping  $L$  constant, we will decrease  $M$  from 1.6 to 1.05. At  $M = M_n^{**}$  (upper branch in Fig. 6) the  $n$ -th eigenfrequency crosses the real  $\omega$  axis and moves into the upper half-plane. The  $n$ -th eigenmode becomes amplified. An important feature of this transition to instability is that the eigenfrequencies do not move towards each other and do not affect each other, that is why we define this transition to instability as “single mode flutter”. With

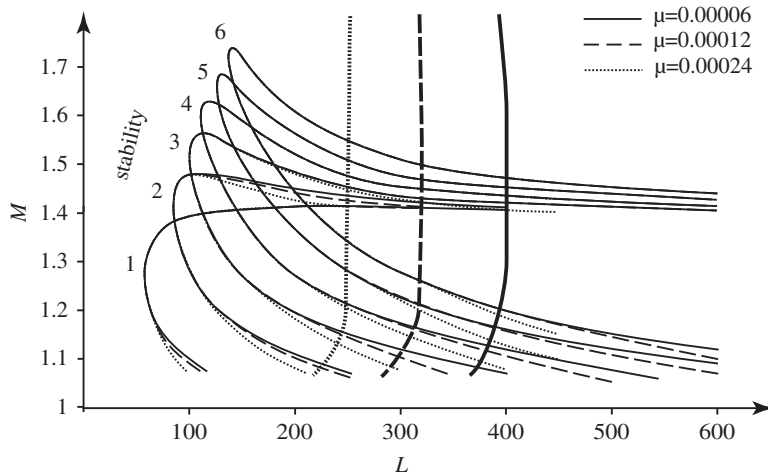


**Fig. 6.** Flutter boundaries in  $M$ – $L$  parameter plane for  $D=23.9$ ,  $M_w=0$ ,  $\mu = 6 \times 10^{-5}$ ,  $12 \times 10^{-5}$ ,  $24 \times 10^{-5}$ . Thin curves: single mode flutter boundaries for modes 1–6, thick curves: coupled mode flutter boundaries.

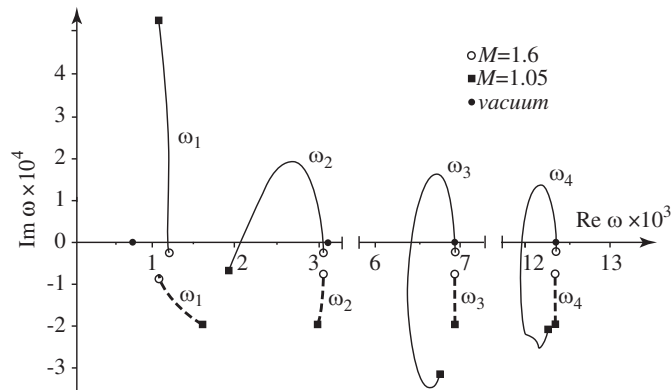


**Fig. 7.** Loci of the first four eigenfrequencies in the complex  $\omega$  plane for parameters (12),  $L=250$ ,  $1.05 \leq M \leq 1.6$ . Continuous and dashed curves represent results obtained through potential flow theory and piston theory, respectively.

further decrease of  $M$ ,  $\text{Im } \omega_n$  get their maxima at decrease. At  $M = M_n^*$  (lower branch in Fig. 6) eigenfrequencies cross the real axis again and move into the lower half-plane; corresponding eigenmodes again become damped. Thus,  $n$ -th eigenmode,  $n = 1, \dots, 4$  is in single mode flutter at  $M_n^* < M < M_n^{**}$ .

Results of calculations using piston theory (8) for  $1.05 < M < 1.6$  are shown in Fig. 7 by dashed curves. There is no transition to instability: all the eigenfrequencies lie in the lower half-plane for any  $M$  from the region  $1.05 < M < 1.6$ . Therefore, piston theory is an inadequate method and cannot be used to investigate or predict the occurrence of single mode flutter.

Let us now consider transition from stability to single mode, and then to coupled mode flutter, with increase of the plate length. Take  $M=1.3$  and increase  $L$  from 60 to 400. In Fig. 8(a) we observe, first, single mode instability, according to crossing of single mode flutter boundary in Fig. 6. Second, at  $L \approx 320$  coalescence of the first and the second eigenfrequencies occurs (saying “coalescence” hereafter, we mean very close approach: eigenfrequencies do not merge exactly, but pass very close to each other). Immediately after coalescence  $\text{Im } \omega_1$  increases very rapidly: from  $4.5 \times 10^{-5}$  at  $L=320$  to  $4.77 \times 10^{-4}$  at  $L=400$ , while  $\text{Im } \omega_2$  decreases: from  $2.8 \times 10^{-5}$  at  $L=320$  to  $-4.08 \times 10^{-4}$  at  $L=400$ . Such behaviour is defined as coupled mode flutter. As transition to coupled mode flutter occurs from the region of single mode flutter, coalescence occurs in the upper  $\omega$ -half-plane (indeed, according to Fig. 6 at  $M=1.3$  and increase of  $L$  we are entering coupled mode flutter region directly from single mode flutter region). Higher eigenfrequencies ( $n > 2$ ) stay in the upper  $\omega$ -half-plane without any approach to each other, thus we observe both coupled mode flutter in the first two eigenmodes, and single mode flutter in higher eigenmodes.

Finally, we will watch motion of the eigenfrequencies in the complex plane during transition from stability directly to coupled mode flutter. Take  $M=1.6$  and increase  $L$ , again from 60 to 400 (Fig. 9(a)). At  $110 \leq L \leq 220$  we observe single mode instability in modes 4, 5, 6, according to crossing of single mode flutter boundaries in Fig. 6; modes 1, 2, 3 are stable while  $L < 321$ . At  $L \approx 321$  the first and the second eigenfrequencies coalesce, however in contrast to  $M=1.3$  case, coalescence occurs in the lower half-plane. After the coalescence  $\text{Im } \omega_1$  increases from  $-2.7 \times 10^{-5}$  at  $L=321$  to  $4.13 \times 10^{-4}$  at  $L=400$ , while

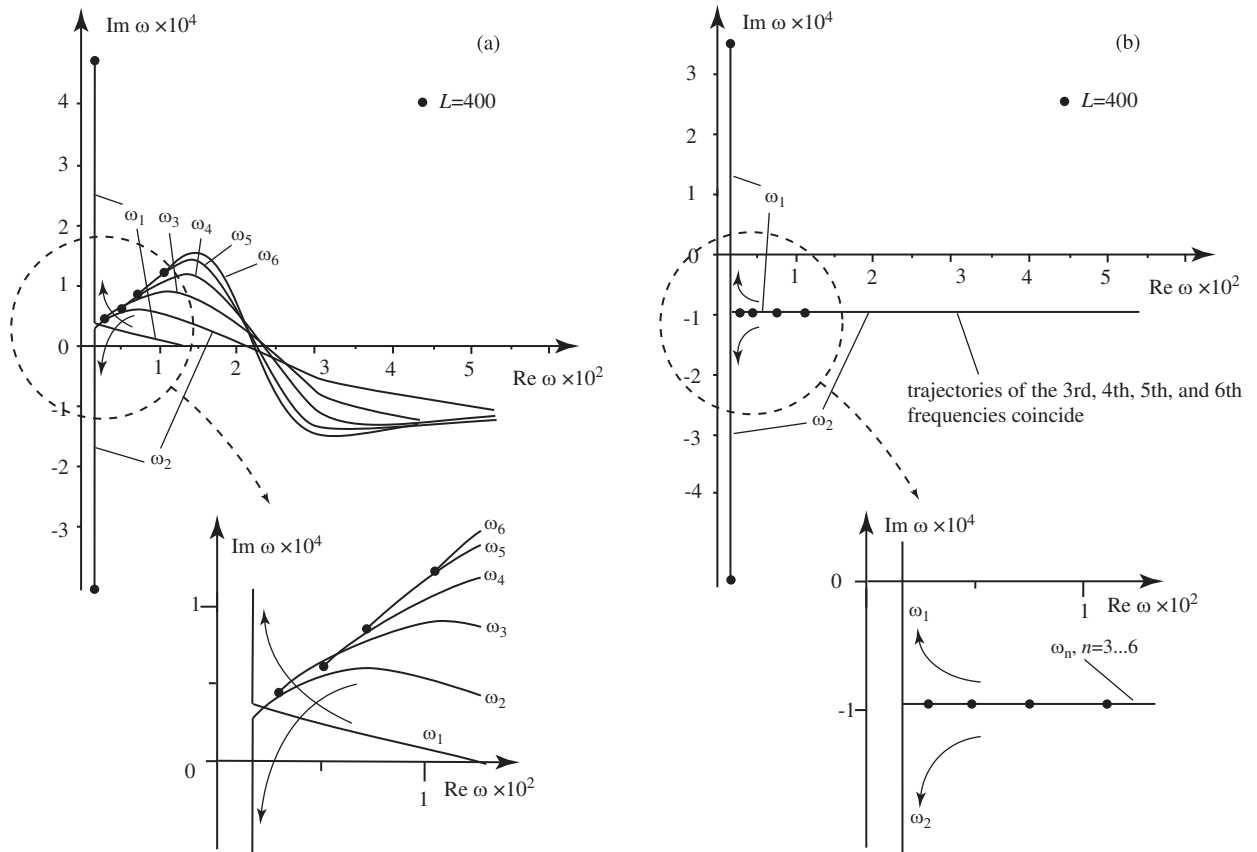


**Fig. 8.** Loci of the first six eigenfrequencies in the complex  $\omega$  plane for parameters (12),  $M=1.3$ ,  $60 \leq L \leq 400$ . (a) Results obtained through potential flow theory; (b) results obtained through piston theory.

$\text{Im } \omega_2$  decreases from  $-2.8 \times 10^{-5}$  at  $L=321$  to  $-4.69 \times 10^{-4}$  at  $L=400$ . Therefore, we observe transition to coupled mode flutter. Other eigenfrequencies ( $n=3, \dots, 6$ ) stay in the lower  $\omega$ -half-plane, therefore those eigenmodes are damped at  $L > 321$ .

Shown in Figs. 8(b) and 9(b) are loci of the eigenfrequencies calculated through piston theory. As before, it is seen that there is no single mode instability, but there is coupled mode instability. Note that coupled mode instability occurs at Mach number, which is very close to the one obtained through potential flow theory.

Another way to observe coupled mode flutter is to increase Mach number. Let us take  $L=300$  and increase  $M$ . Changing  $M$  from 1.05 to 1.6, we pass single mode flutter regions of the first six modes, motion of the eigenfrequencies in the complex plane is qualitatively close to those shown in Fig. 7. Loci of the eigenfrequencies with further increase of  $M$ , up to 2.7, are shown in Fig. 10. At  $M \approx 2.27$  coalescence of the first two eigenfrequencies occurs, and the first one crosses real axis at  $M \approx 2.29$ , almost immediately after the coalescence. Shown by dashed curves in Fig. 10 are loci of the eigenfrequencies, obtained using piston theory. It is seen that results are close to the loci obtained through potential flow theory. Coupled mode instability occurs at  $M \approx 2.30$ , which is very close to  $M \approx 2.29$  from potential flow theory. With further increase of  $M$ , any difference between the eigenfrequencies obtained through piston theory and potential flow theory vanishes. Therefore, piston theory is a very good approximation of the air pressure at high Mach numbers.

Results discussed above concern the first six eigenmodes. From theoretical point of view, we can add single mode flutter boundaries for more and more modes in Fig. 6: according to (16), (17), at least for large  $L$  each mode has its own instability boundary  $M_n^* < M < M_n^{**}$ , where  $M_n^* \rightarrow \infty$ ,  $M_n^{**} \rightarrow \infty$  as  $n \rightarrow \infty$ . In particular, even at higher Mach numbers, such as shown in Fig. 10, there are some higher modes (with  $n > 6$ ) that have positive  $\text{Im } \omega_n$ . However, at very high eigenmodes, single mode flutter cannot occur in actual physical reality. This is due to influence of structural damping action (not considered here), which increases unlimited, whereas  $\text{Im } \omega_n$  is limited as  $n \rightarrow \infty$ .

## 5.2. Influence of $\mu$

As discussed in Section 4, asymptotic single mode flutter boundaries (17) do not depend on  $\mu$ . As  $\mu \rightarrow 0$ ,  $\text{Im } \omega_n$  tends to zero but keeps its sign. On the contrary, influence of  $\mu$  on coupled mode flutter is essential. Indeed, coupled mode flutter occurs due to interaction of two eigenmodes through aerodynamic coupling. This interaction in its turn requires

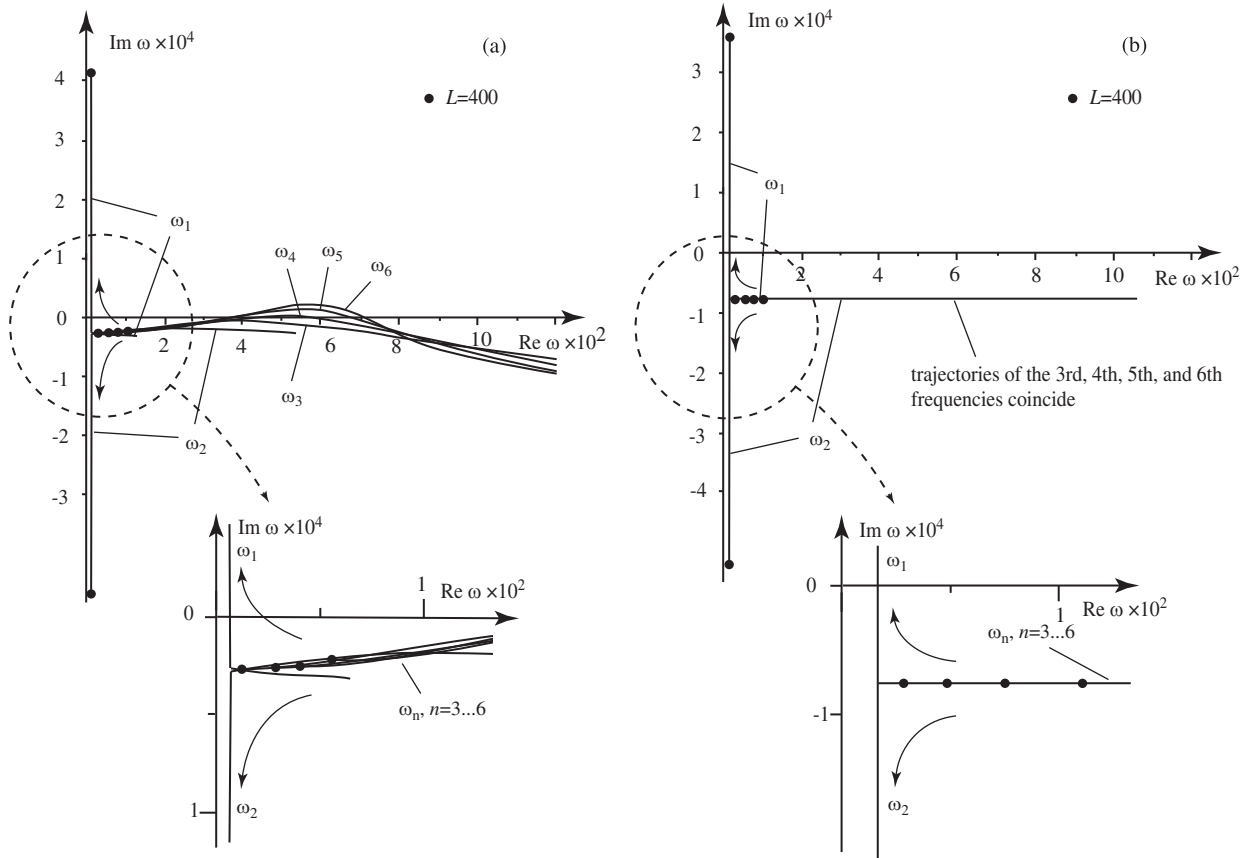


**Fig. 9.** Loci of the first six eigenfrequencies in the complex  $\omega$  plane for parameters (12),  $M=1.6$ ,  $60 \leq L \leq 400$ . (a) Results obtained through potential flow theory; (b) results obtained through piston theory.

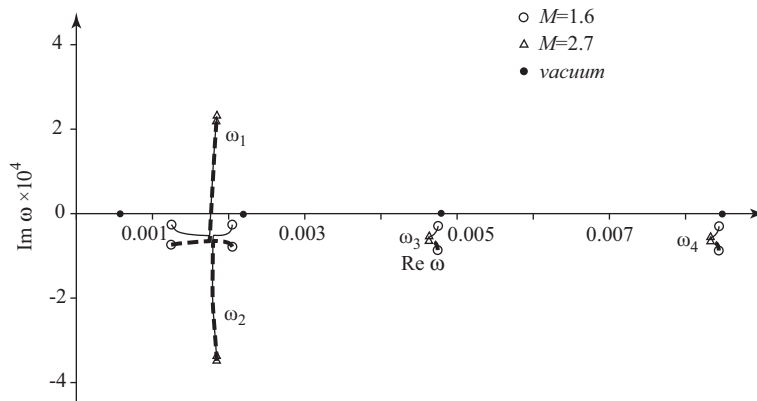


**Fig. 10.** Loci of the first four eigenfrequencies in the complex  $\omega$ -plane for parameters (12),  $L=300$ ,  $1.6 \leq M \leq 2.7$ . Continuous and dashed curves represent results obtained through potential flow theory and piston theory, respectively.

sufficiently high flow density, such that the flow is “strong” enough to significantly move the plate natural frequencies in  $\omega$ -plane. Thus, taking of smaller  $\mu$  results in increase of flutter critical Mach number. In particular, this can be seen from asymptotic coupled mode flutter criterion (18).

Results of calculations fully confirm these considerations. Figs. 6 and 11 show flutter boundaries for parameters  $D=23.9$ ,  $M_w=0$ , and

$$\mu = 6 \times 10^{-5}, \quad 12 \times 10^{-5}, \quad 24 \times 10^{-5}, \quad 48 \times 10^{-5}, \quad 96 \times 10^{-5},$$

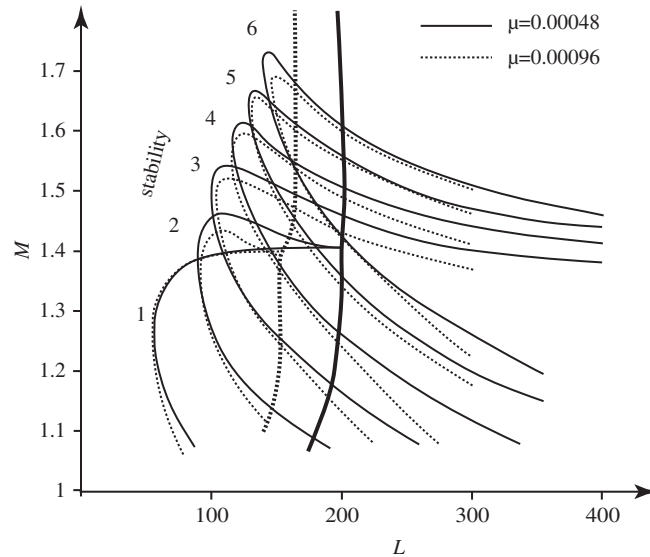


**Fig. 11.** Flutter boundaries in  $M$ – $L$  parameter plane for  $D=23.9$ ,  $M_w=0$ ,  $\mu=48 \times 10^{-5}$ ,  $96 \times 10^{-5}$ . Thin curves: single mode flutter boundaries for modes 1–6, thick curves: coupled mode flutter boundaries.

variation of  $\mu$  corresponds to the following change of the plate material and air densities (from the lowest to the largest  $\mu$ ): steel plate in the air flow at 10 000 m above sea level, steel at 3000 m, titanium at 3000 m, aluminum at 3000 m, carbon composite at 3000 m. Comparing results for  $\mu=6 \times 10^{-5}$ ,  $12 \times 10^{-5}$ , and  $24 \times 10^{-5}$  in Fig. 6, it is seen that difference in single mode flutter boundaries at  $M > 1.25$  is negligible. At  $M < 1.25$  slight influence of  $\mu$  on lower branch of the flutter boundaries appears: lower  $M_n^*$  corresponds to higher  $\mu$ . However, even though  $\mu$  affects flutter boundaries at  $M < 1.25$ , the difference is not really significant.

There is also a minor change of the second mode flutter boundary near intersection point of three boundaries: first mode flutter, second mode flutter, and coupled mode flutter ( $M \approx 1.41$ ). These boundaries intersect in one point, because coincidence of two frequencies at  $\text{Im } \omega = 0$  means that single mode flutter boundaries of coinciding modes also pass through this point. Calculations show that the first mode boundary does not change with  $\mu$ , while second mode boundary slightly deforms to pass through this point. Note that in small neighbourhood of the intersection point the three instability types (first mode, second mode, and coupled mode) are hardly distinguishable, and their boundaries are shown for reference only.

Results for higher  $\mu$  in Fig. 11 show that  $\mu=48 \times 10^{-5}$  and  $96 \times 10^{-5}$  slightly affect single mode flutter boundaries at any  $M$ . However, this influence is still minor: for  $M > 1.25$  difference of upper and lower branches for these  $\mu$  does not exceed  $\Delta M = 0.03$ , while difference along left vertical section of the boundaries does not exceed  $\Delta L = 5$ .

For coupled mode flutter,  $\mu$  is a significant parameter of the flutter boundary. In accordance with considerations above, lower  $\mu$  for the same  $L$  gives less aerodynamic coupling of the modes, which results in higher  $L$  necessary for frequency coalescence and following transition to coupled mode flutter. As  $\mu \rightarrow 0$  and fixed  $L$ , mode coupling disappears (actually moving to much higher  $M$ ), and for any fixed  $M$  the plate becomes stable with respect to coupled mode (but not always to single mode flutter).

It is interesting to note that coupled mode flutter occurs when coupling of the first and second modes takes place. Generally, for higher  $L$  coupling of higher modes also takes place (Movchan, 1957). For  $\mu=6 \times 10^{-5}$  and  $\mu=12 \times 10^{-5}$  such a coupling has not been observed up to  $L=600$ . However, at  $\mu=24 \times 10^{-5}$ ,  $48 \times 10^{-5}$ , and  $96 \times 10^{-5}$  mutual interference of 3, 4, 5 and 6th modes takes place for  $L > 450$ , 350, and 300, respectively. Loci of these eigenfrequencies in the complex plane significantly differ from those shown in Fig. 7, and instability cannot anymore be classified as coupled mode or single mode types. This higher modes coupling, however, is not important from practical point of view, because the plate is already deeply unstable due to coupled mode flutter of the first and second modes. That is why we did not study this behaviour in detail.

### 5.3. Influence of $M_w$ on single mode flutter

According to asymptotic criterion (16), (17), Mach numbers at which the plate flutters significantly increase with increase of  $M_w$ . For example, from (17) it is seen that even for relatively small tension stress  $\sigma = 129.6 \times 10^6$  Pa, flutter critical Mach number  $\min_n M_n^*$  increases from 1.051 for unstressed plate to 1.403. Hereafter parameters

$$D = 23.9, \quad \mu = 12 \times 10^{-5}, \quad (19)$$

**Table 1**  
 Change of single mode flutter boundaries for different in-plane tension, according to asymptotic formulae (17), for parameters (19) as  $L \rightarrow \infty$ .

$\sigma$ (Pa)	$M_w$	$M_n^*$	$M_n^{**}$
0	0.0	1.000	1.414
$8.1 \times 10^6$	0.1	1.100	1.425
$32.4 \times 10^6$	0.2	1.200	1.455
$72.9 \times 10^6$	0.3	1.300	1.502
$129.6 \times 10^6$	0.4	1.400	1.562

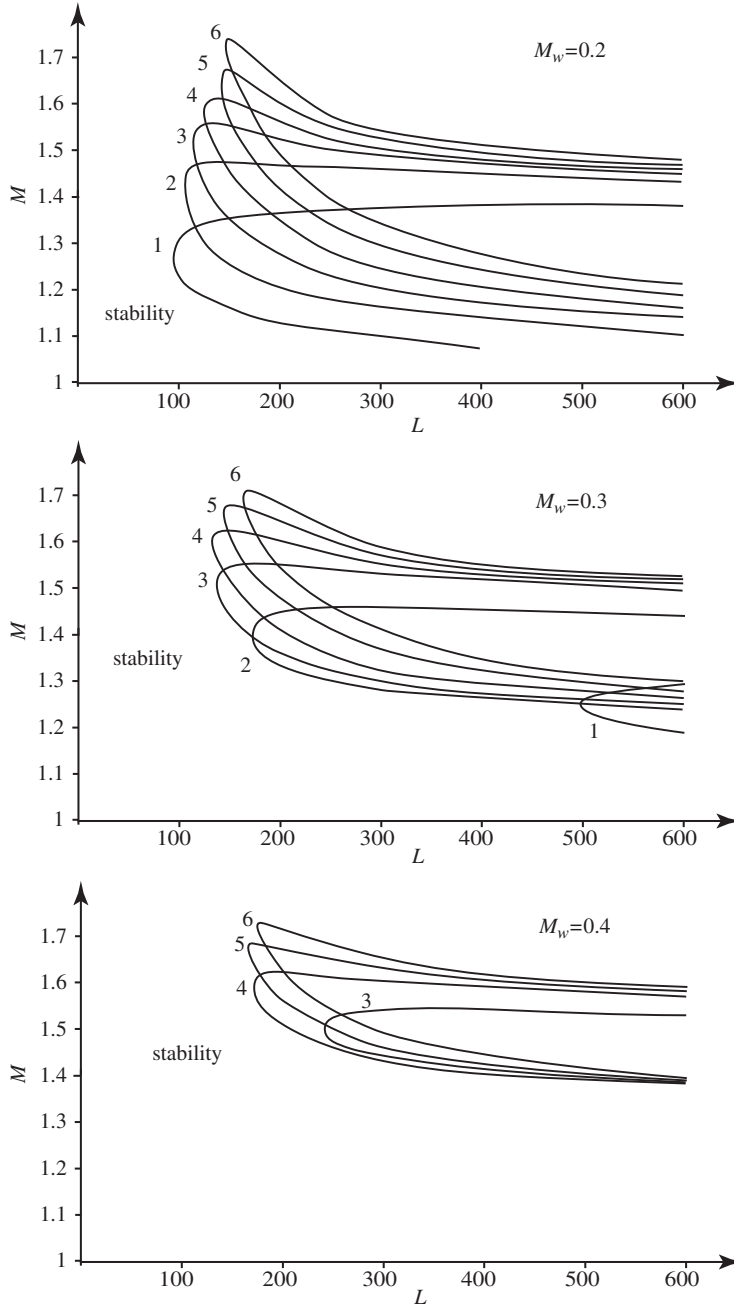


**Fig. 12.** Flutter boundaries of the first six modes in  $M$ – $L$  parameter plane for  $D=23.9$ ,  $M_w=0.2, 0.3, 0.4$ ,  $\mu = 12 \times 10^{-5}$ .

and the plate length  $L=300$  are used in calculations. Shown in Table 1 are upper and lower boundaries obtained from (17) for parameters (19) as  $L \rightarrow \infty$  (dependence of  $M_n^*$ ,  $M_n^{**}$  on  $n$  disappears as  $L \rightarrow \infty$ ).

Results of the numerical study are shown in Fig. 12 for  $M_w=0.2, 0.3$ , and  $0.4$ . First, for  $M_w=0.2$  some change of single mode flutter boundaries is seen, especially for the first mode: upper branch moves down, lower branch moves up, and the left vertical section of the boundary moves right. For other modes, both upper and lower branches move slightly up.

For  $M_w=0.3$  flutter boundary of the first mode moves into the region  $L \geq 500$ , and only very small instability area is observed for  $500 \leq L < 600$ . For the second mode boundary, upper branch moves down, lower branch moves up, left section of the boundary moves right. Instability regions of the third–sixth modes move to higher  $M$  and become narrower.

For  $M_w$  increased up to  $0.4$ , boundaries of both first and second mode move into the region  $L > 600$ , so that they are not in the range of parameters shown in Fig. 12. Instability regions of third–sixth modes move to higher  $M$  and become narrower. Left sections of the third mode flutter boundaries also significantly move to higher  $L$ .

Thus, with increase of  $M_w$  we observe two trends in change of single mode flutter boundaries. First, both lower and upper branches of instability boundaries move to higher  $M$ , which as  $L \rightarrow \infty$  are pretty close to values predicted by the asymptotic formulae (17) (see Table 1). The second trend involves movement of the left sections of lower mode boundaries to a higher  $L$  position, thereby increasing plate lengths at which single mode flutter occurs (this second trend is not covered by the asymptotic theory).

Note that at  $M_w \geq 0.2$  coupled mode flutter boundary moves into the region  $M > 1.8$  for any  $L$ , that is why this boundary does not exist in Fig. 12 (see details in the next section).

#### 5.4. Influence of $M_w$ on coupled mode flutter

In the previous section we studied location of single mode flutter boundaries in the parameter space, when transition to instability occurs without interaction between eigenmodes. At higher  $M$  and  $L$  such a transition occurs through coalescence of eigenfrequencies, producing coupled mode flutter (Fig. 6). From asymptotic theory point of view, this happens when eigenfrequencies of the first modes are located near the vertical section of the curve  $\Omega$  (Fig. 5). This section exists if the condition (18) is satisfied.

Formula (18) gives  $M_w$  of order of  $\mu^{1/3}$ , and as  $\mu$  is typically a small parameter, even relatively small plate tension eliminates coupled mode flutter. Also, (18) does not contain explicitly the plate length  $L$ . This means that taking  $M_w$  such that (18) is not satisfied eliminates coupled mode flutter for any plate of given material, thickness and Mach number range, no matter how long the plate is.

We now consider coupled mode flutter boundaries calculated using potential flow theory, shown in Fig. 13 for parameters (19). For every  $L$ , there is a curve  $M_w = M_w(M)$ , so that we have coupled mode flutter if  $M_w < M_w(M)$ , and no coupled mode flutter otherwise (though single mode flutter is still possible). The curve  $M_w = M_w(M)$ , obtained from asymptotic formula (18), denoted “ $L = \infty$ ”, lies above all the calculated curves for finite  $L$ , and in this sense it is “absolute” coupled mode flutter boundary: taking tension higher than (18), we guarantee stability of a plate of any length.

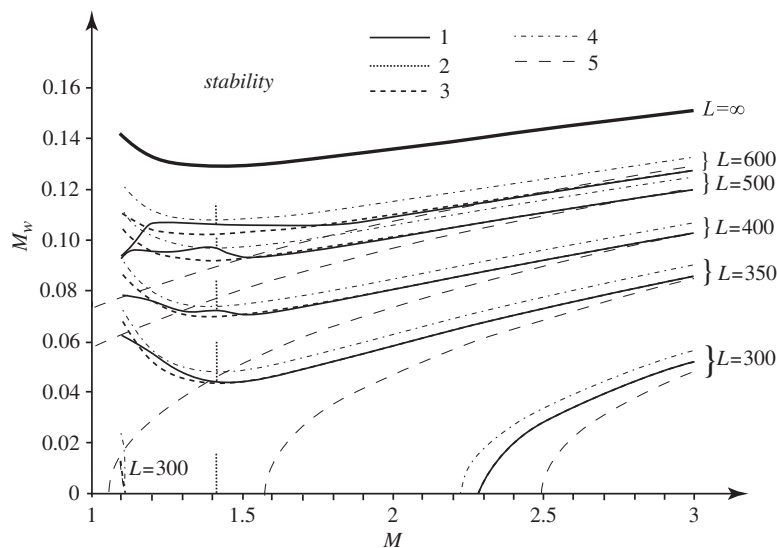


**Fig. 13.** Flutter boundaries of the first two modes in  $M_w$ – $M$  parameter plane for  $D=23.9$ ,  $\mu = 12 \times 10^{-5}$ . 1: coupled mode flutter through potential flow theory, 2: single mode flutter (upper boundary) through potential flow theory, 3: coupled mode flutter through piston theory, 4: coupled mode flutter, formula (21), 5: coupled mode flutter, formula (20). Curve  $L = \infty$  is plotted using (18).

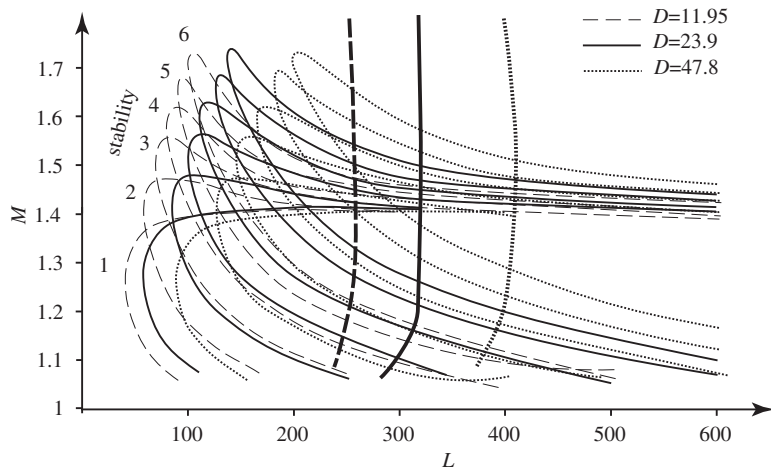


**Fig. 14.** Flutter boundaries in  $M-L$  plane for  $D=11.95, 23.9, 47.8, M_w=0, \mu = 12 \times 10^{-5}$ . Thin curves: single mode flutter boundaries for modes 1–6, thick curves: coupled mode flutter boundaries.

An interesting feature is that one needs much less tension to fully eliminate coupled mode flutter comparing to single mode flutter. Indeed, from Fig. 13 it is seen that  $M_w=0.15$  is enough to avoid coupled mode flutter for any  $L$  up  $M=3.0$ , whereas at  $M_w=0.4$  there is still a region of single mode flutter in Fig. 12 for  $L > 174$  and  $M < 1.74$ .

5.5. Influence of  $D$

Usually panel flutter problem is considered in the context of flight vehicle skin panels. In case of metal panel of aircraft moving in earth’s atmosphere, dependence of dimensionless stiffness  $D$  on the material and the flight altitude is insignificant. The reason is that  $D$  is a function of  $E/\rho_m$  ratio, which does not change much for structural metals, and speed of sound  $a$ , which only slightly depend on the altitude. However, dimensionless stiffness can be essentially different if the panel is made of composite (density is lower, while Young’s modulus in the fibre direction is higher than for metals), or if the flow parameters are different from atmospheric (flows in nozzles of jet and rocket engines, flight vehicles moving in other planet’s atmosphere, etc.). Therefore, study of influence of  $D$  may be useful in some applications.

Shown in Fig. 14 are flutter boundaries for  $M_w=0, \mu = 12 \times 10^{-5}$ , and  $D = 11.95, 23.9, 47.8$ . Main effect of the stiffness increase is shift of the flutter boundaries to the right. Note that coupled mode flutter boundary is shifted more than single mode flutter boundaries, though the shift distances are of the same order. As before, coupled mode flutter boundaries are well approximated by results obtained through piston theory.

6. Comparison of flutter boundaries with other works

Panel flutter problem for simply supported panels has been solved analytically by Movchan (1957). The following sufficient stability condition has been obtained (we use notations of the present paper):

$$M < \frac{D}{\mu L^3} \frac{8\pi^3}{3\sqrt{3}} \left( 5 + \frac{L^2 M_w^2}{2\pi^2 D} \right) \sqrt{2 + \frac{L^2 M_w^2}{2\pi^2 D}} \tag{20}$$

Movchan used this version of piston theory:

$$p\{W, \omega\} = \mu \left( -i\omega W(x) + M \frac{dW(x)}{dx} \right).$$

Comparing this formula with (8) and considering that coefficient of  $dW(x)/dx$  is responsible for coupled mode instability, we conclude that sufficient stability condition obtained through (8) can be derived from (20) by changing  $M$  to  $M^2/\sqrt{M^2-1}$ :

$$\frac{M^2}{\sqrt{M^2-1}} < \frac{D}{\mu L^3} \frac{8\pi^3}{3\sqrt{3}} \left( 5 + \frac{L^2 M_w^2}{2\pi^2 D} \right) \sqrt{2 + \frac{L^2 M_w^2}{2\pi^2 D}} \tag{21}$$

Results of calculations using (20) and (21) are shown in Fig. 13. It is seen that sufficient stability condition (20) is a good approximation of exact coupled mode flutter boundary at  $M > 2.5$ ; this was pointed out by Movchan (1957). Fig. 13 also shows that modification (21) correctly predicts coupled mode flutter boundary in much wider range, even at low  $M > 1.1$ , where piston theory of any modification is, strictly speaking, inadequate. Therefore, we conclude that piston theory in

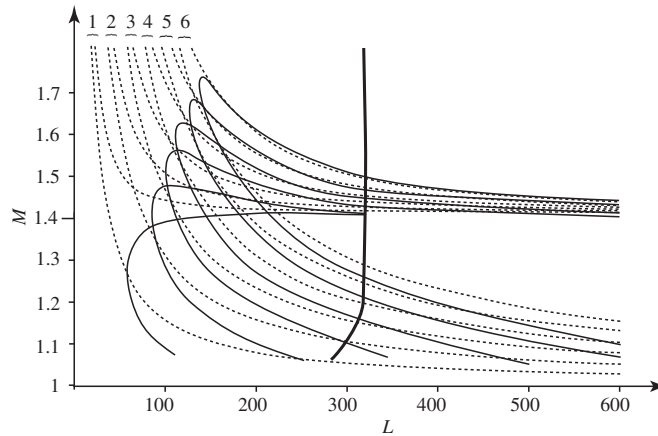


Fig. 15. Numerical (continuous curves) and asymptotic (dashed curves) flutter boundaries for modes 1–6 for parameters (12).

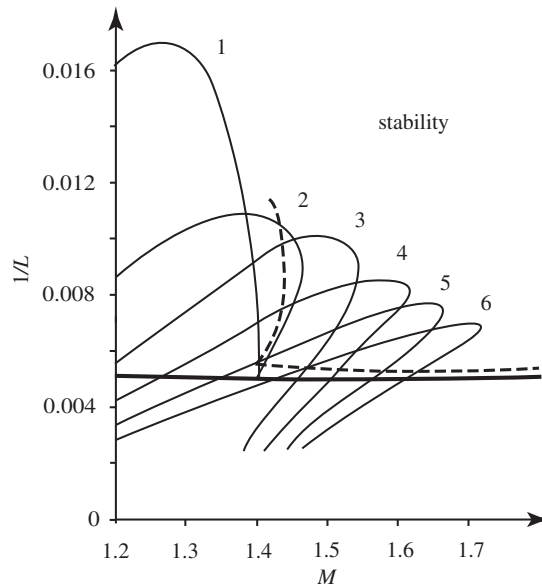


Fig. 16. Single mode flutter boundaries for modes 1–6 (thin continuous curves), coupled mode flutter boundary (thick continuous curve) for aluminium panel at sea level; Nelson and Cunningham's results (dashed curve, from their Fig. 12).

form (21), and only in this particular form, accurately predicts frequency coalescence at any  $M > 1.1$ , though being inapplicable to prediction of single mode flutter.

It is also interesting to note that for long plates, limit of (21) as  $L \rightarrow \infty$  exactly coincides with asymptotic coupled mode flutter criterion (18), obtained using Kulikovskii's theory of global instability.

Let us now compare single mode flutter boundaries. First, in Fig. 15 comparison of exact (calculated herein) and asymptotic boundaries (17) is shown. Two differences are obvious. First, exact boundaries have minimum in  $L$ , while asymptotic boundaries, according to (17), extend to  $L=0$  (meanwhile,  $M_n^*(L), M_n^{**}(L) \rightarrow \infty$ ). Second, exact  $M_n^*(L)$  are slightly lower than the asymptotic ones. This difference is smaller for higher mode number  $n$ . Upper boundaries  $M_n^{**}(L)$  are in excellent agreement.

Linear flutter boundaries of finite simply supported plate through potential flow theory were studied by Nelson and Cunningham (1956), results are presented in their Fig. 12. They studied aluminium panel at sea level; dimensional parameters are  $E = 7 \times 10^{10}$  Pa,  $\nu = 0.3$ ,  $\rho_m = 2700$  kg/m<sup>3</sup>,  $a = 340.3$  m/s,  $\rho = 1.225$  kg/m<sup>3</sup>. Corresponding dimensionless parameters are as follows:

$$D = 20.5, \quad M_w = 0, \quad \mu = 45.4 \times 10^{-5}.$$

Closest parameters available for comparison in the present study are

$$D = 23.9, \quad M_w = 0, \quad \mu = 48 \times 10^{-5}.$$

Corresponding flutter boundaries from Fig. 11 are compared with Nelson and Cunningham's results in Fig. 16 in terms of  $1/L$  versus  $M$ . It is seen that Nelson and Cunningham's horizontal section of the boundary corresponds to coupled mode flutter; their vertical section corresponds to single mode flutter in the second mode. Higher modes are not presented in their study, as they used two-mode Galerkin approximation. From Fig. 16 it is seen that flutter in higher modes essentially widens whole instability region of the panel.

Also, several nonlinear studies are available for comparison. First, Dowell (1967) reported that single mode flutter in the first mode has been observed for  $M < \sqrt{2}$  for a very small dynamic pressure, which in notations of the present paper is equivalent to very small  $\mu$ . At  $M > \sqrt{2}$  direct transition to coupled mode flutter occurred, with no higher modes oscillations.

However, Bendiksen and Davis (1995) (also reported by Bendiksen and Seber, 2008) observed transition from single mode flutter in the first mode at  $M=1.2$  to oscillations in several higher modes simultaneously at  $M=1.4$ ; shape of the plate deflection was changing with time from the fourth to the fifth mode shape and vice versa. At  $M=1.5$ , single mode oscillations in the fifth mode only were detected. Such a behaviour was explained by possible influence of "aerodynamic or simply numerical noise", however results of the present paper show that most likely the authors observed single mode flutter in higher modes.

## 7. Conclusions

Flutter boundaries of simply supported plates have been studied using potential flow theory. Two types of flutter have been observed: coupled mode and single mode flutter. Coupled mode flutter boundaries are in full agreement with known results obtained using piston theory for  $M \gg 1$ . It has been shown that piston theory in form (8), or, equivalently, (2), correctly predicts coupled mode flutter boundaries even for low supersonic Mach numbers ( $1.1 < M < 1.7$ ).

In contrast to coupled mode flutter, single mode flutter cannot be investigated using piston theory. In fact, piston theory has been found to be inadequate to analyze or to predict the single mode flutter. It has been shown that this type of flutter can occur in several modes simultaneously. Meanwhile, each mode has its own flutter region in the parameter space. For the first mode this region (in the case of an unstressed plate) is typically in  $1 < M < \sqrt{2}$ ; however, for higher modes single mode flutter occurs at higher Mach numbers, up to  $M \approx 1.75$  for the sixth mode (for the parameters studied herein). Flutter regions of higher modes are located in higher Mach number range. Theoretically, for any  $M > 1$ , when given a plate of appropriate length, there exists an eigenmode, which is unstable at this  $M$ , and the actual occurrence of this flutter in physical reality is only limited by the structural damping properties of the plate, and its nonlinear properties.

For plates pre-stressed by in-plane tension, single mode flutter boundary for each mode shifts to a higher range of  $M$ . At the same time, in  $M$ - $L$  parameter plane, flutter regions of lower modes move to higher  $L$  region.

The occurrence of single mode flutter is not influenced by gas density. This means that panel exposure to varying gas types of differing density will result in no (or insignificant) changes to the flutter boundaries. In contrast, the phenomenon of coupled mode flutter is highly influenced by gas density.

From a practical standpoint, the most important aspect of single mode flutter is to recognize that this flutter phenomenon can occur at lower Mach numbers and for shorter plate conditions; thereby it is able to exist at conditions where the occurrence of coupled mode flutter would be impossible. Typical aeroelastic analysis methods using piston theory are inadequate to investigate or predict the occurrence of single mode flutter. Therefore, aeroelastic analysis that relies solely upon piston theory for investigative study, can neglect the occurrence of single mode flutter, leading to the potential for fatigue damage and destruction of skin panels on a flight vehicle.

## Acknowledgement

The work is supported by Russian Foundation for Basic Research (projects 10-01-00256 and 11-01-00034).

## References

- Abdel-Motagaly, K., Chen, R., Mei, C., 1999. Nonlinear flutter of composite panels under yawed supersonic flow using finite elements. *AIAA Journal* 37 (9), 1025–1032.
- Banichuk, N., Jeronen, J., Neittaanmäki, P., Tuovinen, T., 2011. Dynamic behaviour of an axially moving plate undergoing small cylindrical deformation submerged in axially flowing ideal fluid. *Journal of Fluids and Structures* 27, 986–1005.
- Bendiksen, O.O., Davis, G.A., 1995. Nonlinear Traveling Wave Flutter of Panels in Transonic Flow. *AIAA Paper* 95-1486, p. 17.
- Bendiksen, O.O., Seber, G., 2008. Fluid-structure interactions with both structural and fluid nonlinearities. *Journal of Sound and Vibration* 315 (3), 664–684.
- Bohon, H.L., 1963. Flutter of Flat Rectangular Orthotropic Panels with Biaxial Loading and Arbitrary Flow Direction. NASA TN D-1949.
- Bolotin, V.V., 1960. Nonlinear flutter of plates and shells. *Inzhenernyi Sbornik* 28, 55–75 (in Russian).
- Bolotin, V.V., 1963. *Nonconservative Problems of the Theory of Elastic Stability*. Pergamon Press, Oxford.

- Bolotin, V.V., Grishko, A.A., Kounadis, A.N., Gantes, C., Roberts, J.B., 1998. Influence of initial conditions on the postcritical behavior of a nonlinear aeroelastic system. *Nonlinear Dynamics* 15, 63–81.
- Doaré, O., de Langre, E., 2006. The role of boundary conditions in the instability of one-dimensional systems. *European Journal of Mechanics B/Fluids* 25 (6), 948–959.
- Dong Ming-de, 1984. Eigenvalue problem for integro-differential equation of supersonic panel flutter. *Applied Mathematics and Mechanics* 5 (1), 1029–1040.
- Dowell, E.H., 1966. Nonlinear oscillations of fluttering plate. *AIAA Journal* 4 (7), 1267–1275.
- Dowell, E.H., 1967. Nonlinear oscillations of fluttering plate. II. *AIAA Journal* 5 (10), 1856–1862.
- Dowell, E.H., 1971. Generalized aerodynamic forces on a flexible plate undergoing transient motion in a shear flow with an application to panel flutter. *AIAA Journal* 9 (5), 834–841.
- Dowell, E.H., 1974. *Aeroelasticity of Plates and Shells*. Noordhoff International Publishing, Leyden.
- Dowell, E.H., 1982. Flutter of a buckled plate as an example of chaotic motion of a deterministic autonomous system. *Journal of Sound and Vibration* 85 (3), 330–344.
- Dowell, E.H., Voss, H.M., 1965. Theoretical and experimental panel flutter studies in the Mach number range 1.0 to 5.0. *AIAA Journal* 3 (12), 2292–2304.
- Duan, B., Abdel-Motagaly, K., Guo, X., Mei, C., 2003. Suppression of Supersonic Panel Flutter and Thermal Deflection using Shape Memory Alloy. *AIAA Paper* 2003-1513.
- Dugundji, J., 1966. Theoretical considerations of panel flutter at high supersonic Mach numbers. *AIAA Journal* 4 (7), 1257–1266.
- Dun Min-de, 1958. On the stability of elastic plates in a supersonic stream. *Soviet Physics Doklady* 3, 479–482.
- Garric, I.E., Rubinow, S.E., 1946. Flutter and Oscillating Air-Force Calculations for an Airfoil in a Two-Dimensional Supersonic Flow. *NACA Report No. 846*.
- Gordnier, R.E., Visbal, M.R., 2001. Computation of Three-Dimensional Nonlinear Panel Flutter. *AIAA Paper* 2001-0571, p. 17.
- Hashimoto, A., Aoyama, T., Nakamura, Y., 2009. Effect of turbulent boundary layer on panel flutter. *AIAA Journal* 47 (12), 2785–2791.
- Hedgepeth, J.M., 1957. Flutter of rectangular simply supported panels at high supersonic speeds. *Journal of the Aeronautical Sciences* 24 (8), 563–573 586.
- Kulikovskii, A.G., 1966. On the stability of homogeneous states. *Journal of Applied Mathematics and Mechanics* 30 (1), 180–187.
- Kulikovskii, A.G., 2006. The global instability of uniform flows in non-one-dimensional regions. *Journal of Applied Mathematics and Mechanics* 70 (2), 229–234.
- Mei, C., Abdel-Motagaly, K., Chen, R.R., 1999. Review of nonlinear panel flutter at supersonic and hypersonic speeds. *Applied Mechanics Reviews* 10, 321–332.
- Miles, J.W., 1959. *The Potential Theory of Unsteady Supersonic Flow*. Cambridge University Press, Cambridge.
- Movchan, A.A., 1956. On oscillations of a plate moving in a gas. *Prikladnaya Matematika i Mekhanika* 20 (2), 211–222 (in Russian).
- Movchan, A.A., 1957. On stability of a panel moving in a gas. *Prikladnaya Matematika i Mekhanika* 21 (2), 231–243 (in Russian, translated in NASA RE 11-22-58 W, 1959).
- Nelson, H.C., Cunningham, H.J., 1956. Theoretical Investigation of Flutter of Two-Dimensional Flat Panels with One Surface Exposed to Supersonic Potential Flow. *NACA Report No. 1280*.
- Peake, N., 2004. On the unsteady motion of a long fluid-loaded elastic plate with mean flow. *Journal of Fluid Mechanics* 507, 335–366.
- Selvam, R.P., Visbal, M.R., Morton, S.A., 1998. Computation of Nonlinear Viscous Panel Flutter Using a Fully-Implicit Aeroelastic Solver. *AIAA Paper* 98-1844, p. 10.
- Vedeneev, V.V., 2005. Flutter of a wide strip plate in a supersonic gas flow. *Fluid Dynamics* 5, 805–817.
- Vedeneev, V.V., 2006. High-frequency flutter of a rectangular plate. *Fluid Dynamics* 4, 641–648.
- Vedeneev, V.V., 2007. Nonlinear high-frequency flutter of a plate. *Fluid Dynamics* 5, 858–868.
- Vedeneev, V.V., Guvernyuk, S.V., Zubkov, A.F., Kolotnikov, M.E., 2010. Experimental observation of single mode panel flutter in supersonic gas flow. *Journal of Fluids and Structures* 26, 764–779.
- Yang, T.Y., 1975. Flutter of flat finite element panels in supersonic potential flow. *AIAA Journal* 13 (11), 1502–1507.
- Zhou, R.C., Lai, Z., Xue, D.Y., Huang, J.-K., Mei, C., 1995. Suppression of nonlinear panel flutter with piezoelectric actuators using finite element method. *AIAA Journal* 33 (6), 1098–1105.